

APPLICATION OF GEOGRAPHICAL INFORMATION SYSTEM FOR MAPPING FIRE RISK AND DESIGNING FOREST ROADS

Aidin Parsakhoo

Department of Forestry, Faculty of Forest Science, Gorgan University of Agricultural Sciences and Natural Resources, P. Box 386, Gorgan, Iran. E-mail: Aidinparsakhoo@yahoo.com

Received: 05 May 2014

Accepted: 11 June 2014

Abstract

Fires are one of the most important disturbances in forests and they damage them. This study was conducted to classify fire risk for a deciduous forest and to predict the locations of forest stands for which fire control operations are required. Normalized Difference Vegetation Index (*NDVI*) and Moisture Vegetation Index (*MVI*) were extracted from satellite imagery of *IRS LISS III* and *Landsat 7 ETM+*, respectively. Altitude, slope aspect and slope gradient maps were obtained from a digital elevation model using surface analysis in ArcMap. Buffers were created from 0 to 300, 300 to 600, 600 to 900 meters and over 900 meters along the road and around the cattle pens as zones with different levels of fire risk. All the thematic layers were then integrated using the overlay procedure in GIS. Results from the analytical hierarchy process showed that vegetation indices were given the largest weight. The influence of slope gradient on fire behavior was assessed the third largest weight. Slope aspect was assigned the same weight as to slope gradient. The distance from roads and cattle-pens was evaluated with the fourth largest weight. 25 % of the forest area is classified as area with very high degree of vulnerability to fire. This class is generally distributed in the entire region, while areas with very low fire risk are found in the northern parts.

Key words: AHP, GIS, fire risk map, Hyrcanian forest, satellite imagery.

Introduction

One of the main causes of destruction in recent years are wildfires (Gromtsev 2002). The growth of seasonal temperatures also has increased the number of spontaneous wildfires in the predominantly forested areas (Köse et al. 2008). Forest fires are responsible for some devastating damages such as loss of biodiversity, reduction of forests, alteration of landscape, soil degradation, increase in the greenhouse effect, etc (Tuia et al. 2008). The forest fire could influence the

soil micro arthropod assemblage in two ways: directly killing by the blaze and indirectly – altering the arthropods' habitat by changing the composition of forest vegetation or disturbing the balance of soil chemicals, water levels, and soil pH. In addition, burning out of leaf litter and other organic matter may cause the depletion of food source of soil arthropods since decomposers are closely associated with those organic substrates (Kim and Jung 2008). In Turkey, forest fires are still one of the greatest natural hazard problems. Last six decades,

1.504.245 ha of forests has been affected by fire (Chuvienco and Salas 1996). Smith et al. (2005) showed that, in the case of Savanna fires, surface spectral reflectance increases with the increasing of fire severity due to the formation of increasing quantities of white mineral ash. Also, their studies showed linear relationships between fire duration and post-fire surface spectral reflectance, with the optimal relationship being a ratio of the 450 and 2034 nm spectral reflectance observations.

The effects of fire on forest ecosystems are different according to their characteristics (Bowmana et al. 2008). But in general, by determining the fire risk zone, the type of fire and its intensity, the duration, size, power and the season in which it has occurred, it is possible to control fire damage (Podur et al. 2002, Fulé et al. 2008). The most common fires in Mazandaran natural resources in Hyrcanian zone of Iran are small (less than 0.5 hectare) and superficial, caused by people (unintentionally). Local distribution of fires in the province show that fire frequency in the province increases from east to west. In 2006, 49.36 % of all fires have occurred just in Sari, Neka and Behshahr. The analogical share in 2005 was 73.82 %. Therefore, governments should use funds from their fire suppression budgets for fire alert activities. Early warning systems should keep the population aware of the risk of fires in critical periods, and the use of open fires should be absolutely prohibited (Ritchie et al. 2007).

The regime of fires Fire regime in the Hyrcanian deciduous forests is poorly understood but it has been largely inferred by the fire traits history. In the present study, an attempt was made to prepare a forest map of fire risk zones by integrating

a satellite image, topographic and other thematic maps from a geographic information system (GIS) for the Miana forest which is covering the sensitive to forest fires areas in Iran.

Materials and Methods

Description of the study area

Measurements were carried out in the Miana forest which is situated in the deciduous northern forested part of Iran from $52^{\circ}56'30''$ to $52^{\circ}59'25''$ East longitude and from $36^{\circ}12'25''$ to $36^{\circ}16'35''$ North latitude. A Digital Elevation Model (DEM) was generated with 20-m resolution in ArcMap (Figure 1). Annual

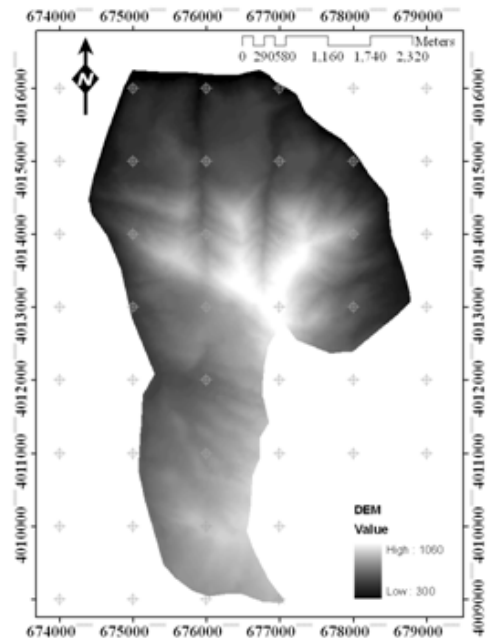


Fig. 1. DEM of the study area.

mean temperature ranges from +12 °C to +14 °C. Annual mean precipitation is between 900 and 1000 mm. The forest altitude ranges from 320 to 1060 m above sea level. Soil textures range from loam to loamy silt and loamy clay. The study area is covered by four kinds of soils, namely non development randzin, washed brown soil with calsic horizon, calcareous brown soil and brown with alkaline soil pH. The bed rock is limestone, calcareous sandstone, marl lime and calcareous conglomerate. The total area of the Miana forest is 1831 hectares. In 1996 a 10800 m long road was provided for this area.

Vegetation indices values

In Normalized Difference Vegetation Index (*NDVI*), the ratio between red (*RED*) and near-infrared (*NIR*) bands is used to em-

phasize the spectral differences between these bands, showing vegetation conditions (Figure 2a). The *NDVI* was calculated using Equation (1).

$$NDVI = (NIR - RED)/(NIR + RED) \quad (1)$$

Where *NIR* is near infrared band (Band 4) and *R* is red band (Band 3) of the *IRS* LISS III digital image. The spatial resolution of *IRS* images was 23.5 m and band lengths corresponded to the green, red, near infrared and middle infrared. Landsat 7 ETM+ images with 30 m spatial resolution were used to obtain Moisture Vegetation Index (*MVI*). Using the mid-infrared (*MIR*) band, which is characteristic with lower atmospheric scattering, instead of the red band, may produce higher correlations to vegetation targets on land surface (Equation 2).

$$MVI = (NIR - MIR)/(NIR + MIR) \quad (2)$$

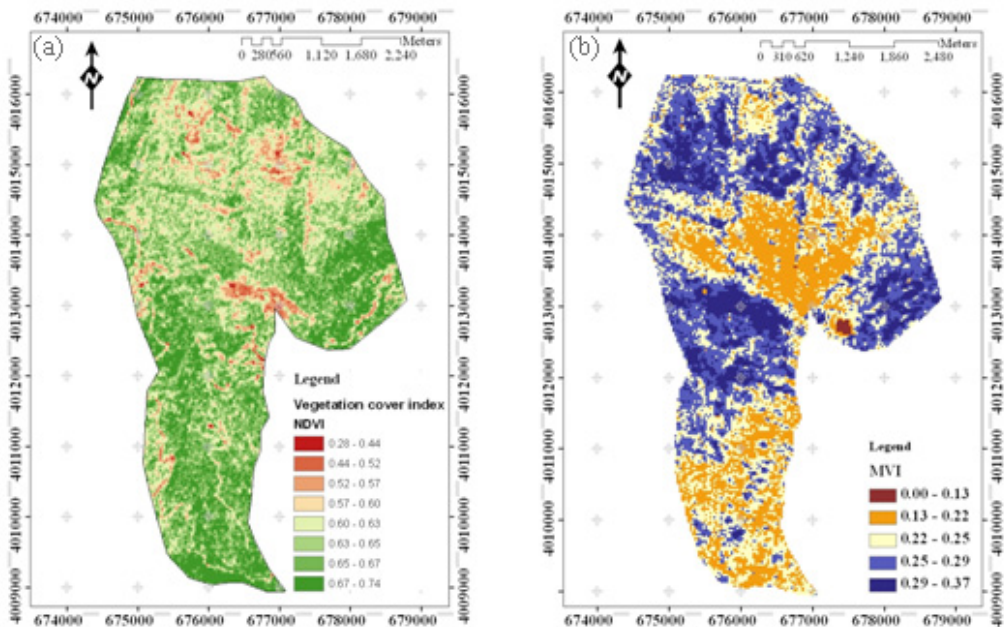


Fig. 2.t Maps of the study area: (a) *NDVI* and (b) *MVI*.

Where *MIR* is middle infrared band (Band 5) and *R* is red band (Band 4) of ETM+ sensor (Figure 2b).

Topography

Altitude (Figure 3a), slope aspect (Figure 3b) and slope gradient (Figure 3c) maps

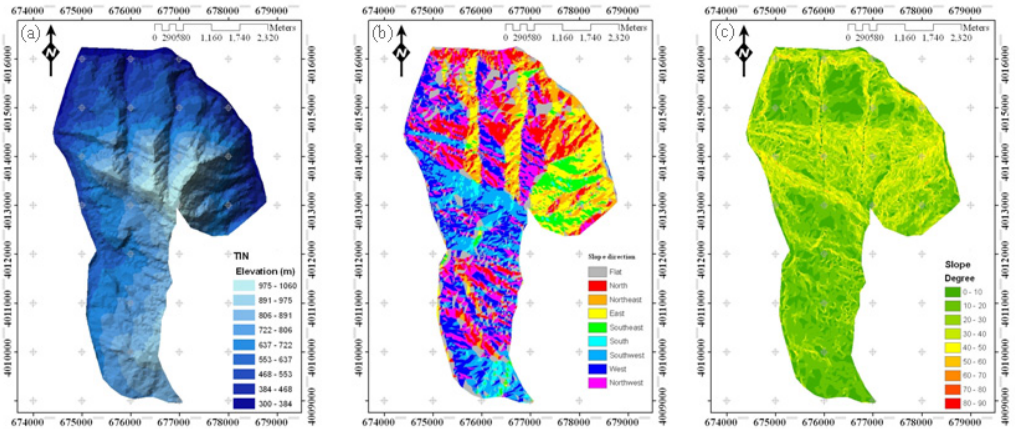


Fig. 3. (a) Altitude, (b) slope aspect and (c) slope gradient maps of the study area.

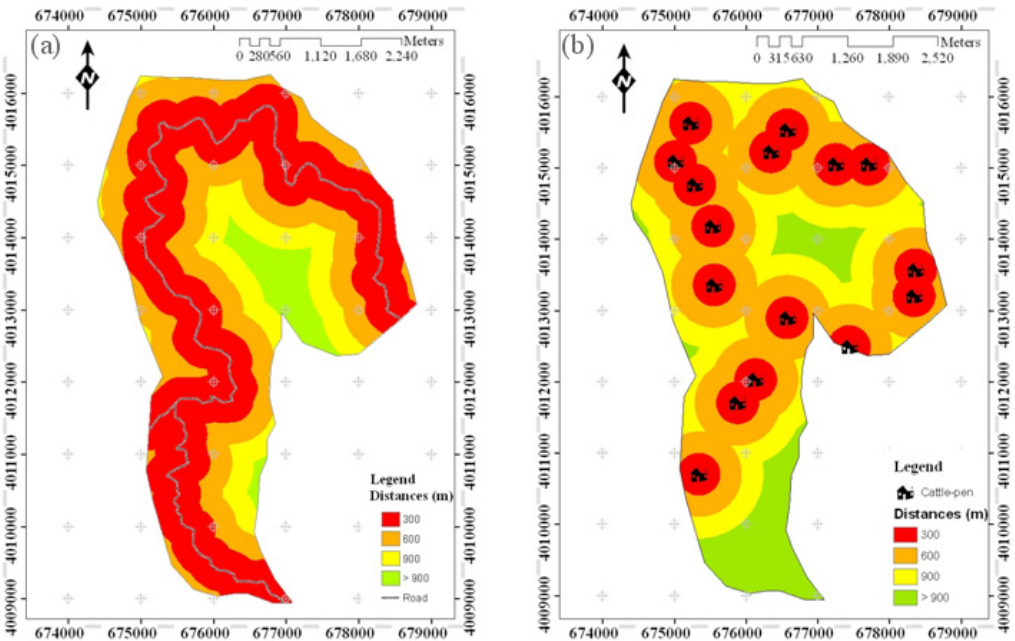


Fig. 4. (a) Road corridor and (b) cattle-pen buffer maps of the study area.

were obtained from the digital elevation model using surface analysis in ArcMap.

Distance from roads and cattle-pens

Forests can be burned in result of the movement of people, animals and vehicles. Thus, forests that are close to roads and cattle-pens are fire prone. Buffers were created from 0 to 300, 300 to 600, 600 to 900 meters and over 900 meters along the road and around the cattle-pens as zones with different levels of fire risk. ArcMap was used for creating such buffer zones along the road (Figure 4a) and around the cattle-pens (Figure 4b).

Determination of factor weights and risk degrees

Expert choice software version 9.5 was used for analytical hierarchy process (Expert Choice Inc 1995). AHP is based on determining the relative priorities of the criteria by pairwise comparison. In this research, by adopting AHP technique with integrating expert opinions, weights of effective factors are quantified by assigning a value from 0 to 9. All the thematic layers were then integrated using the overlay process of GIS. ArcGIS version 9.2 and IDRISI Andes version 15.0 software packages were utilized as basic analysis tools for spatial analysis and data layers manipulation. The equation used in GIS to determine forest fire risk places is:

$$FR = 0.366 V_M + 0.256 V_D + 0.121(S_D + S_S) + 0.057 (D_R + D_C) + 0.022 E \quad (3)$$

Results

Over 75 % of the total area was represented by areas with vegetation moisture index more than 0.22 (Figure 5). The study area has been covered by forest trees, shrubs

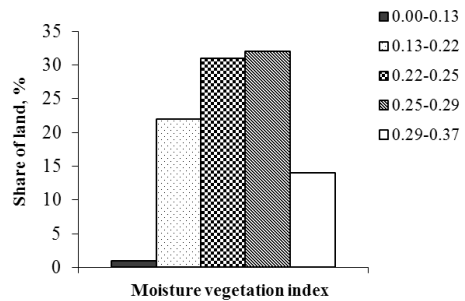


Fig. 5. Distribution of lands covered by different MVI classes.

and herbaceous, so the largest part of the region's area has received NDVI values greater than 0.5 (Figure 6).

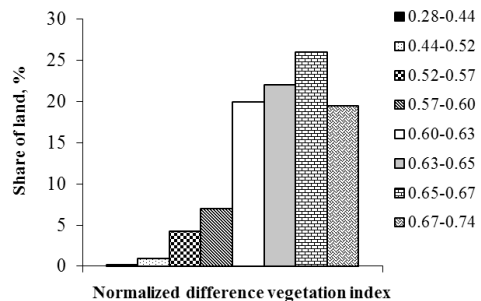


Fig. 6. Distribution of lands covered by different NDVI classes.

Over 70 % of the total area was represented by areas within the altitude range 468–891 meters (Figure 7). The study area includes slopes with all kinds of aspects (Figure 8). The general slope gradient of Miana forest is less than 50 % (Figure 9). Approximately 50 % of the total area is

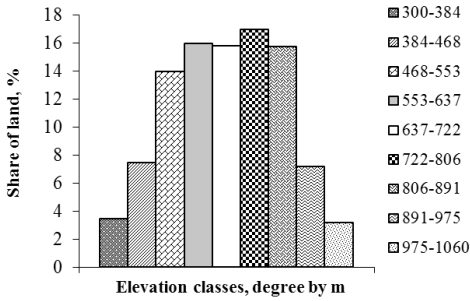


Fig. 7. Distribution of lands in different altitude classes.

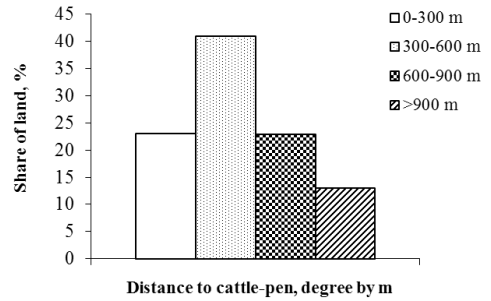


Fig. 10. Distribution of lands by different distances to road.

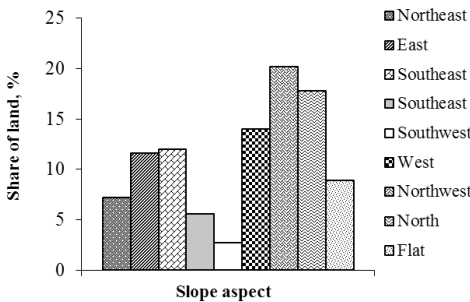


Fig. 8. Distribution of lands in different slope aspects.

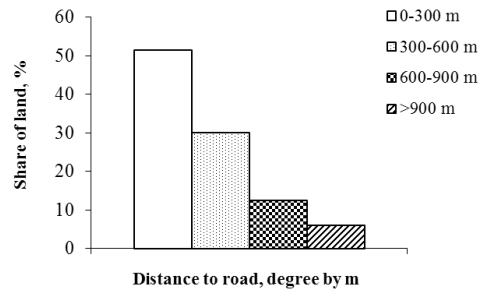


Fig. 11. Distribution of lands by different distances to cattle-pens.

within a distance of up to 300 meters from the road (Figure 10). Less than 25 % of the

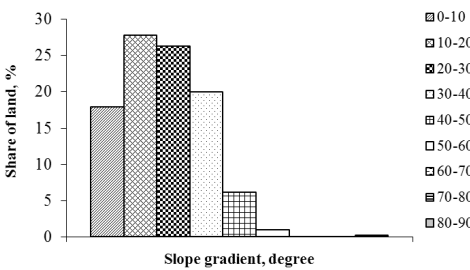


Fig. 9. Distribution of lands in different slope gradient classes.

total area was represented by areas closer than 300 meters to cattle-pens (Figure 11).

During the analysis, vegetation moisture and of vegetation cover have been assigned the greatest weights because even though an environment may be favourable for a wildfire, fire cannot occur unless fuel is available and vegetation is dry. The impact of slope gradient on fire behaviour was evaluated with the third largest weight. Aspect was assigned equal weight with slope gradient. Since the sunlight is much more reflected by southern slopes, fire breaks out fast and spreads over the southern slopes. Distance from roads and cattle-pens was rated with the fourth largest weight. The risk factor decreases with

increasing distance to these objects. It means that zones that are closer to these places were given a higher rating (Table 1).

The priority as an effective factor for fire occurrence in forests has the plant and soil moisture (0.366) > vegetation cover (0.256) > slope gradient = slope direction (0.121) > distance to cattle pen and road (0.057) > altitude (0.023) (Figure

12). 25 % of the forest area is classified as such with very high vulnerability to fire. This class is generally distributed in the entire region, while areas with very low risk are found in the northern parts (Figure 13). Road designing was done according to the forest fire risk map (Figure 14). Characteristics of forest road networks have been shown in Table 2.

Table 1. Weights and ratings assigned to variables and classes for forest fire risk modeling.

Variables	Classes	Ratings	Variables	Classes	Ratings
Moisture of vegetation cover (weight = 0.366)	0.00–0.13	8	Distance to road in meters (weight = 0.057)	0–300	8
	0.13–0.22	7		300–600	6
	0.22–0.25	6		600–900	4
	0.25–0.29	5		> 900	2
	0.29–0.37	4			
Vegetation cover (weight = 0.256)	0.28–0.44	2	Distance to cattle-pens in meters (weight = 0.057)	0–300	8
	0.44–0.52	3		300–600	6
	0.52–0.57	4		600–900	4
	0.57–0.60	5		> 900	2
	0.60–0.63	6	Flat	1	
	0.63–0.65	7	North	2	
Altitude in meters (weight = 0.022)	0.65–0.67	8	Slope aspect (weight = 0.121)	North east	3
	0.67–0.74	9		East	4
	975–1060	1		North west	5
	891–975	2		West	6
	806–891	3		South east	7
	722–806	4		South west	8
	637–722	5		South	9
	553–637	6		0–10	1
468–553	7	10–20	2		
Map of fire risk	384–468	8	Slope gradient in degrees (weight = 0.121)	20–30	3
	3.2–4.6	Very low		30–40	4
	4.6–5.2	Low		40–50	5
	5.2–5.7	Moderate		50–60	6
	5.7–6.2	High		60–70	7
	6.2–7.4	Very high		70–80	8
			80–90	9	

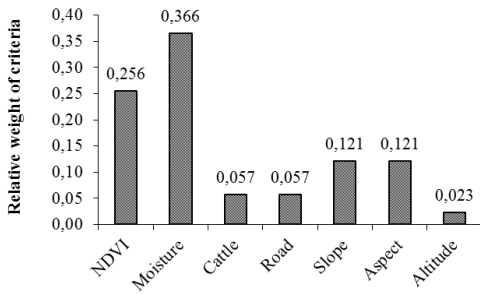


Fig. 12. Derived priorities with respect to effective factors on forest fire.
Note: Inconsistency Ratio = 0.05.

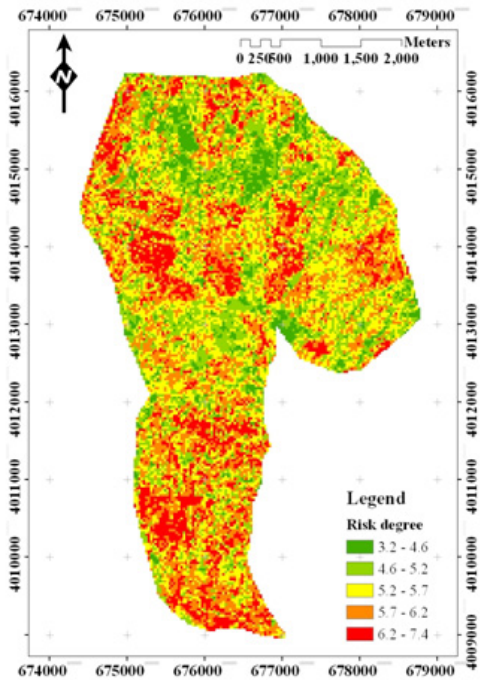


Fig. 13. Forest fire risk map.

Table 2. Technical characteristics of forest road network.

Road density, m·ha ⁻¹	Road spacing, m	Skidding distance, m	Road performance, %
14	714	357	63

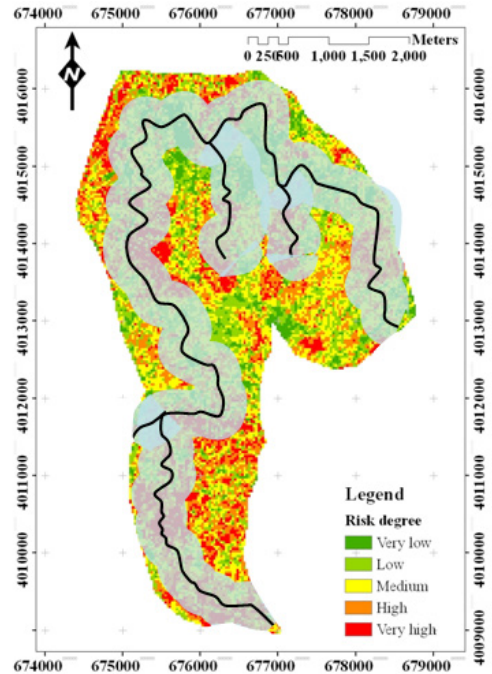


Fig. 14. Designing of access roads to fire risk zone.

Discussion

The use of satellite imagery to measure the impact of fire on vegetation communities has become a popular topic of discussion in recent years (Gromtsev 1996). It has been demonstrated that a relationship between fire severity and soil damage can be deduced in eucalypt forests by fire severity measures an important finding for understanding the interrelationship between wildfire, soil erosion and water quality (Sriboonpong et al. 2001, Shakesby et al. 2007). Zhijun et al. (2009) in a study in Jeilin province of China applied satellite data and GIS techniques to provide new layers from effective factors for forest sensitivity to fire. They showed that the most important effective factor for

a start of a fire is topography and human activity, respectively.

Forest fire risk zones are locations where a fire is likely to start, and from where it can easily spread to other areas (Breece et al. 2008). Anticipation of factors influencing the occurrence of fire and understanding the dynamic behaviour of fire are critical aspects of fire management (Jaiswal et al. 2002). A geographic information system (GIS) can be used effectively to combine different forest-fire causing factors for demanding the forest fire risk zone map (Robert et al. 2001). *MVI* show best performances in dense humid forests, whereas *NDVI* is a good indicator of green biomass in deciduous and dry forests (Marozas et al. 2007). Satellite data are suitable instruments to introduce and classify forest places when integrating the parameters topography, vegetation cover, vicinity to roads and settlements (Tapias et al. 2004). The integration of this satellite data into GIS can be very useful to determine risky places and to plan forestry management after fire (Erten et al. 2005).

Angayarkkani and Radhakrishnan (2010) have presented an intelligent system for effective forest fire detection using spatial data. The proposed system made use of image processing and artificial intelligence techniques. The images in the spatial data, obtained from remote sensing, have been utilized by the presented system for the detection of forest fires. GIS is very useful and important in forest fire management. GIS plays a critical role in mapping and documenting fire, predicting its course, analyzing alternative fire-fighting strategies, and directing tactics and strategies in the field. GIS can make the information possible to be an input for decisions by establishing a rela-

tion among the information (Chuvieco and Congalton 1989).

Conclusion

Minute and complete assessment of fire damages in forests and estimating the starting spread of a fire are possible using a map of forest fire risk zones. This map is produced by integrating satellite images in the data base of a geographic information system (GIS). In this way, collected data include a topographic map, a vegetation map, maps of slope gradient and aspect. Distance from cattle-pens and roads, have been used for understanding the behavior of forest fires and establishing locations where a fire is likely to start and from where it can easily spread to other areas. Therefore, it is necessary to determine the fire risk zones for all forest sites and use these data for a better planning and managing of forests. The experimental results have demonstrated the effectiveness of the proposed integrated system in detecting forest fires using spatial data.

References

- ANGAYARKKANI K., RADHAKRISHNAN N. 2010. An intelligent system for effective forest fire detection using spatial data. *International Journal of Computer Science and Information Security* 7: 202–208.
- BREECE C.R., KOLB T.E., DICKSON B.G., McMILLIN J.D., CLANCY K.M. 2008. Prescribed fire effects on bark beetle activity and tree mortality in southwestern ponderosa pine forests. *Forest Ecology and Management* 255: 1190–128.
- BOWMANA M.S., AMACHERA G.S., MERRY F.D. 2008. Fire use and prevention by traditional

households in the Brazilian Amazon. *Ecological Economics* 67: 117–130.

CHUVIECO E., CONGALTON R.G. 1989. Application of remote sensing and geographic information systems to forest fire hazard mapping. *Remote Sensing of the Environment* 29: 147–159.

CHUVIECO E., SALAS J. 1996. Mapping the spatial distribution of forest fire danger using GIS. *International Journal of Geology Information System* 10: 333–345.

GROMTSEV A.N. 1996. Retrospective analysis of natural fire regimes in landscapes of Eastern Fennoscandia and problem of their anthropogenic transformation. In: Goldammer: 45–54.

GROMTSEV A.N. 2002. Natural disturbance dynamics in the boreal forests of European Russia: a review. *Silva Fennica* 36: 41–55.

ERTEN E., KURGUN V., MUSAOLU N. 2005. Forest fire risk zone mapping from satellite imagery and GIS a case study. *Civil Engineering Faculty, Remote Sensing Division* 7 p.

FULÉ P.Z., RIBAS M., GUTIÉRREZ E., VALLEJO R., KAYE M.W. 2008. Forest structure and fire history in an old *Pinus nigra* forest, eastern Spain. *Forest Ecology and Management* 255: 1234–1242.

JAISWAL R.K., MUKHERJEE S., RAJU D.K., SAXENA R. 2002. Forest fire risk zone mapping from satellite imagery and GIS. *International Journal of Applied Earth Observation and Geo information* 4: 1–10.

KÖSE K., GRAMMALIDIS N., YILMAZ E.E., CETIN E. 2008. 3D wildfire simulation system. *The International Archives of the Photogrammetry, Remote Sensing and Spatial Information Sciences*. Vol. XXXVII. Part B8. Beijing: 1431–1436.

KIM J.W., JUNG C. 2008. Abundance of soil microarthropods associated with forest fire severity in Samcheok. *Journal of Asia-Pacific Entomology* 11: 77–81.

MAROZAS V., RACINSKAS J., BARTKEVICIUS E. 2007. Dynamics of ground vegetation after surface fires in hemiboreal *Pinus sylvestris* forests. *Forest Ecology and Management* 241: 47–55.

PODUR J., MARTELL D.L., KNIGHT K. 2002. Statistical quality control analysis of forest fire activity in Canada. *Canadian Journal Forest Research* 32: 195–205.

RITCHIE M.W., SKINNER C.N., HAMILTON T.A. 2007. Probability of tree survival after wildfire in an interior pine forest of northern California: Effects of thinning and prescribed fire. *Forest Ecology and Management* 247: 200–208.

ROBERT E.K., BURGAN R., WAGTENDONK J.V. 2001. Mapping wildland fuels for fire management across multiple scales: Integrating remote sensing, GIS, and biophysical modeling. *International Journal of Wildland Fire* 10: 301–319.

SHAKESBY R.A., WALLBRINK P.J., DOERR S., ENGLISH P., CHAFER C.J., HUMPHREYS G., TOMKINS K. 2007. Distinctiveness of wildfire effects on soil erosion in southeast Australian eucalypt forests assessed in a global context. *Forest Ecology and Management* 238: 347–364.

SMITH A.M., WOOSTER M.J., DRAKE N., DIPOSTO F., FALKOWSKI M., HUDAK A.T. 2005. Testing the potential of multi-spectral remote sensing for retrospectively estimating fire severity in African Savanna environments. *Remote Sensing of Environment* 97: 92–115.

SRIBOONPONG S., HUSSIN Y.A., GIER A. 2001. Assessment of forest recovery after fire using LANDSAT TM images and GIS techniques: A case study of Mae Wong national park, Thailand. 22nd Asian conference on Remote Sensing, 5–9 November 2001, Singapore, 6 p.

TAPIAS R., CLIMENT J.A., PARDOS L. 2004. Life histories of Mediterranean pines. *Plant Ecology* 171: 53–68.

TUIA D., RATLE F., LASAPONARA R., TELESKA L., KANEVSKI M. 2008. Scan statistics analysis of forest fire clusters. *Communications in Nonlinear Science and Numerical Simulation* 13: 1689–1694.

ZHIJUN T., JIQUAN Z., XINGPENG L. 2009. GIS-based risk assessment of grassland fire disaster in western Jilin province, China. *Stochastic Environmental Research and Risk Assessment* 23: 463–471.